

## Properties of the $^{209}\text{Bi}$ Ground-State Analog in $^{209}\text{Po}^\dagger$

G. M. Crawley, W. Benenson, P. S. Miller, D. L. Bayer, and R. St. Onge  
*Cyclotron Laboratory, Michigan State University, East Lansing, Michigan 48823*  
 and

A. Kromminga

*Calvin College, Grand Rapids, Michigan 49506*

(Received 16 February 1970)

The analog of the ground state of  $^{208}\text{Bi}$  was investigated by both the  $^{208}\text{Bi}(p,n)^{208}\text{Po}$  and the  $^{208}\text{Bi}(p,\bar{n})^{208}\text{Bi}$  reactions. The Coulomb energy difference  $^{208}\text{Po}-^{208}\text{Bi}$  was determined as  $18.92 \pm 0.03$  MeV, and the relative partial widths for proton decay into the  $p_{1/2}$ ,  $f_{5/2}$ , and  $p_{3/2}$  channels were determined. The total width of the analog state was found to be  $380 \pm 80$  keV.

### 1. INTRODUCTION

The nuclei near the magic numbers  $Z = 82$  and  $N = 126$  have been the subject of numerous shell-model studies, and it is generally concluded that the low-lying states can be described by fairly simple configurations. For example, various stripping reactions have shown that  $^{207}\text{Pb}$  has a number of pure hole states in the  $^{208}\text{Pb}$  core.<sup>1</sup> The low-lying levels of  $^{208}\text{Bi}$  have also been treated as quite pure particle-hole configurations.<sup>2</sup> Both the positions of the levels, and stripping and pickup reactions<sup>3,4</sup> are consistent with small admixtures between various multiplets.

In addition, the analog of the ground states of many of the nuclei in this mass region have been observed as resonances in proton elastic and inelastic scattering, and their positions and widths have been extracted.<sup>5-8</sup> Information on the  $T = T_z + 1$  analog of the ground state of  $^{208}\text{Pb}$  has also been obtained recently from the reaction  $^{208}\text{Pb}(p, \bar{n})$ .<sup>9</sup>

The experiment described in this paper exploits the  $(p, \bar{n})$  reaction<sup>10-12</sup> to study the analog of the  $^{209}\text{Bi}$  ground state in the nucleus  $^{209}\text{Po}$ . This particular state cannot be readily studied by a resonance method, since the  $^{208}\text{Bi}$  target is unstable, with a half-life of  $3.7 \times 10^5$  yr. Since the  $\bar{p}$  spectrum contains a number of peaks due to the multiplet structure of  $^{208}\text{Bi}$ , the direct  $(p, n)$  measurement of the analog state was also undertaken to check its position and width. Additional information on the partial widths for proton decay of the analog state was also obtained.

### 2. EXPERIMENT

The  $^{209}\text{Bi}(p, \bar{n})$  experiment was carried out using the extracted beam from the Michigan State University isochronous cyclotron at proton energies from 24 to 30 MeV. The protons were detected in a counter telescope of cooled silicon surface-barri-

er detectors. Protons were separated from other reaction products using the program TOOTSIE<sup>13</sup> in an XDS Sigma 7 computer. Spectra were taken at 90, 120, and 160° to check the kinematic effects on the line shape of the protons emitted from the analog state and to check the isotropy of the emitted protons. Isotropy is expected if the  $(p, n)$  reaction goes by simple charge exchange, since the isospin lowering operator  $T^-$  does not affect the population of magnetic substates in the nucleus.

A spectrum taken at 160° and at 24.7-MeV bombarding energy is shown in Fig. 1. The striking feature of this spectrum is the three peaks observed at a proton energy of about 11 MeV. These peaks were shown to remain at about the same absolute energy for a number of bombarding energies between 24 and 30 MeV.

The energy scale of the detector was calibrated using the inelastically scattered protons from a thin carbon foil. Calibration runs were made before and after each  $\bar{p}$  run. While the energy of the protons from the decay of the analog state is independent of the bombarding energy, the absolute calibration of the detector depends upon the calibration of the energy-analysis magnets in the beam transport system. This uncertainty is believed to be less than 50 keV<sup>14</sup> for 25-MeV protons.

The target thickness also contributes to the uncertainty in the position of the  $\bar{p}$  peak. Fortunately this could be calculated, since  $^{209}\text{Bi}(p, d)^{208}\text{Bi}$  spectra were taken at the same time as the  $\bar{p}$  runs and so from the width of the deuteron peaks (which was essentially due to target thickness), the target thickness for the protons could be calculated to within  $\pm 10$  keV.

The kinematic corrections are more difficult to establish since the distribution of the velocities of the  $^{209}\text{Po}$  recoil nuclei following the  $(p, n)$  reaction gives rise to both a shift and a broadening of the  $\bar{p}$  spectrum. The magnitudes of these effects depend

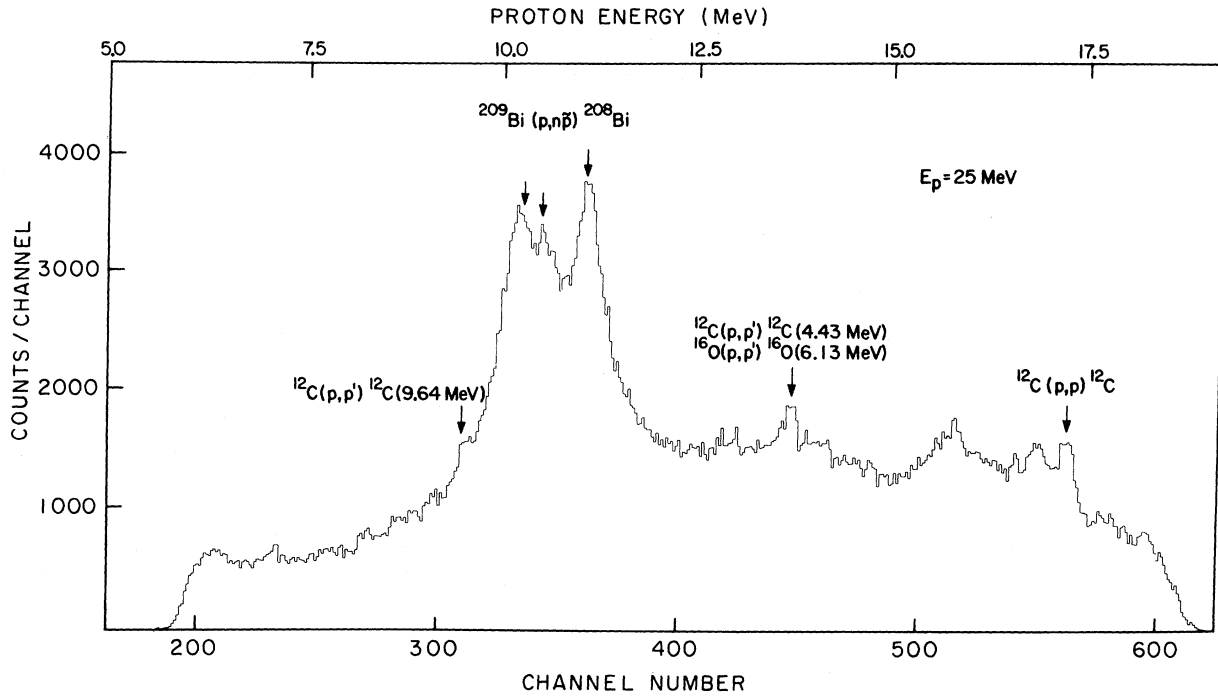


FIG. 1. Spectrum of protons scattered from  $^{209}\text{Bi}$  at a laboratory angle of  $160^\circ$ . The suppression of the spectrum below channel 200 and above channel 600 is instrumental, corresponding to the detector thickness used.

upon the angular distribution of the neutrons and the  $\bar{p}$  detection angle. There is an additional constant energy shift in the lab system because of the recoil caused by proton emission.

A summary of these effects, assuming three different neutron distributions (labeled 1, 2, and 3), is shown in Fig. 2. When the protons are detected at  $90^\circ$ , the centroid of the  $\bar{p}$  peak is the same as  $E_C$ , the lab energy obtained if the  $^{209}\text{Po}$  nucleus decayed at rest, regardless of the neutron angular distribution. The decay energy was therefore calculated from the spectra measured at  $90^\circ$ . The observed difference in energy between the  $90$  and  $160^\circ$  spectra, shown also in Fig. 2 implies that the  $(p, n)$  angular distribution for the analog state is forward peaked, although the detailed distribution cannot be uniquely determined.

Figure 3 gives a comparison of the calculated  $\bar{p}$  line shapes at  $90$  and  $160^\circ$  for the three  $(p, n)$  angular distributions shown in Fig. 2. The curves are normalized to have the same area. A very narrow intrinsic width for the analog state of  $10$  keV was chosen in the calculation so that the details of the line shape could be seen. The extreme distributions 1 and 3 give line shapes with essentially the same width at both angles. Distribution 2, which resembles most measured angular distributions, gives a full width at half maximum of  $80$  keV at  $90^\circ$  and  $35$  keV at  $160^\circ$ . The width is a maximum near

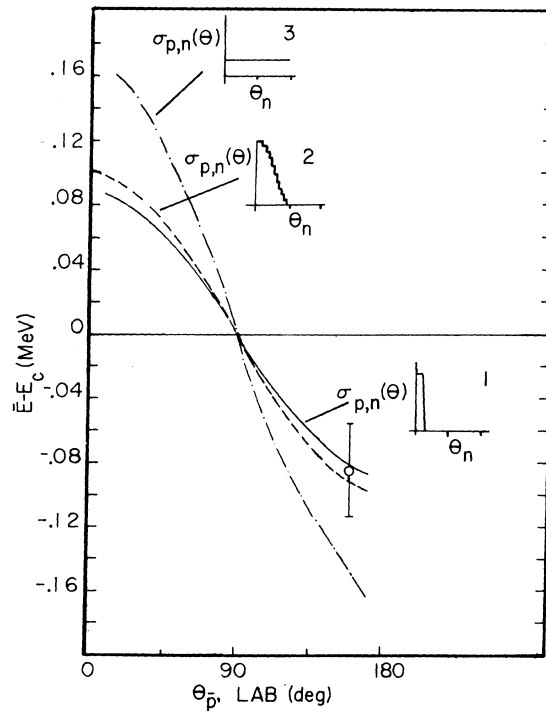


FIG. 2. Dependence of the proton centroid energy  $\bar{E}$  on the detection angle calculated for the three  $(p, n)$  angular distributions shown.  $E_C = 208/209 E_p$  (c.m.), where  $E_p$  (c.m.) is defined in Eq. (1).

$90^\circ$  for any moderately forward-peaked distribution. However, the magnitude of the effect is small compared to the observed width of the peaks, and only introduces a small error in the width of the analog state.

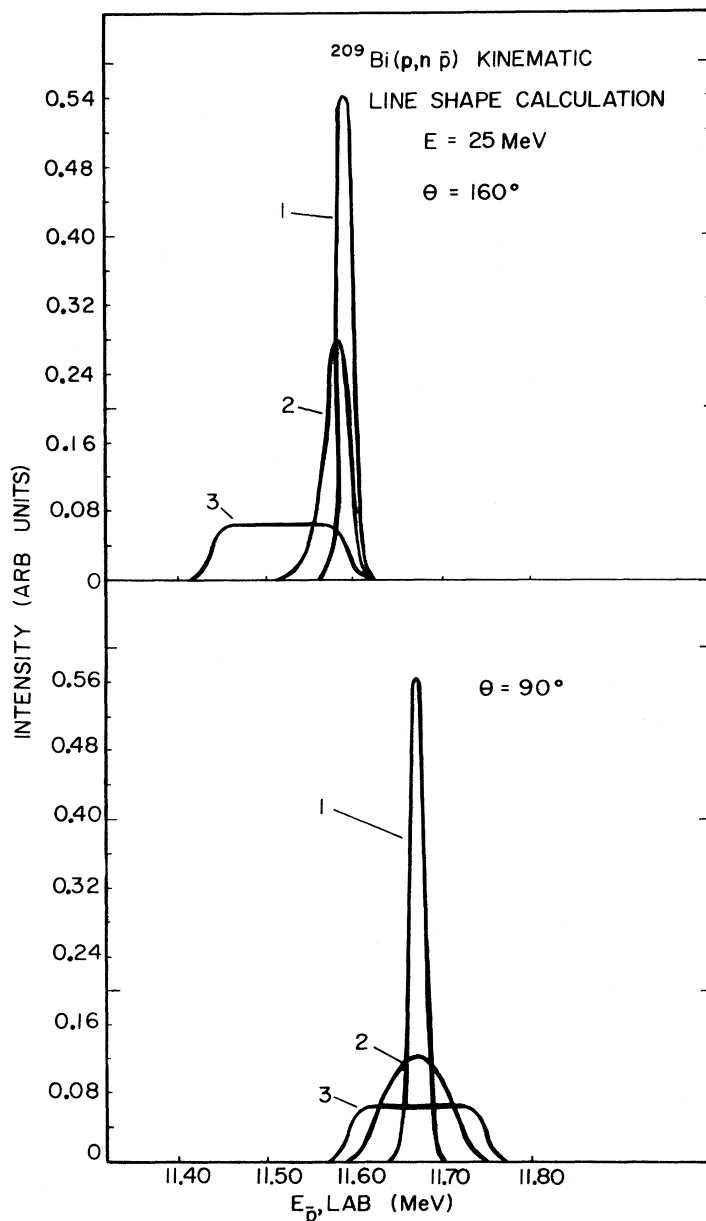
It should be noted that the curves in Fig. 3 were calculated for a Coulomb energy difference of 19.18 MeV, which is higher than the value observed. These curves therefore peak at correspondingly higher energies than the experimental spectra.

The determination of the energy of the analog state is further complicated by the fact that the proton decay proceeds to closely spaced multiplets in  $^{208}\text{Bi}$ . Even the ground-state multiplet

consists of two states 60 keV apart.<sup>2</sup> Therefore, as an independent check on the position and width of the analog state, the direct  $(p, n)$  measurement was made.

Neutrons were detected in a 5-in. plastic scintillator about 5 m from the Bi target.  $\gamma$ -ray discrimination was improved by displaying the pulse-shape-discriminator output versus light output as a two-dimensional display in the Sigma 7 computer and using the program TOOTSIE<sup>13</sup> to allow for curvature in the  $\gamma$ -ray and neutron lines. The neutron time-of-flight spectrum was taken using a time-to-amplitude converter. The intrinsic time resolution of the system was 1.5 nsec. The  $^{209}\text{Bi}(p, n)$

FIG. 3. Calculation of line shapes at lab angles of  $90^\circ$  and  $160^\circ$  for various  $(p, n)$  angular distributions. Note that the intrinsic line-width is assumed to be 10 keV to illustrate the effects clearly.



spectrum showed only one large neutron peak at the energy of the analog state. The energy calibration was obtained from the  $^{12}\text{C}(p, n)^{12}\text{N}$  reaction. The results were quite consistent with the  $\bar{p}$  data.

### 3. COULOMB ENERGY DIFFERENCES

The energy of the delayed protons to the ground state of  $^{208}\text{Bi}$  was determined as 11.409 MeV with an error of 30 keV due to the finite width of the state and the effect of the 60-keV doublet in  $^{208}\text{Bi}$ . The Coulomb energy difference between  $^{209}\text{Po}$  and  $^{209}\text{Bi}$  is then obtained from the equation

$$\Delta E_C = E_p(\text{c.m.}) + B_n(^{209}\text{Bi}), \quad (1)$$

where  $B_n$  is the binding energy of the last neutron in  $^{209}\text{Bi}$ .<sup>15</sup> After making the c.m. correction, the Coulomb energy difference was obtained as 18.917 MeV  $\pm$  33 keV. While this is the first measurement of the Po-Bi Coulomb energy difference, it is interesting to compare it with the  $^{209}\text{Bi}$ - $^{209}\text{Pb}$  values obtained previously. These results are shown in Table I. Although the effect of the extra proton is to increase the Coulomb energy by 110  $\pm$  40 keV, one might have expected an increase of nearly 300 keV from the formula<sup>16</sup>

$$\Delta E_C = 1.443 \bar{Z}/A^{1/3} - 1.12 \text{ MeV}. \quad (2)$$

However, even a simple model of the states which includes the Coulomb interaction of particles in shells outside the  $^{208}\text{Pb}$  core indicates that this value could easily be much smaller than 300 keV. A discussion of the many effects which arise in a more accurate calculation has been given by Auerbach *et al.*<sup>17</sup>

### 4. THEORY AND DISCUSSION

The low-lying states in  $^{208}\text{Bi}$  arise from particle-hole couplings which form closely spaced multiplets, and it is assumed that there are no admix-

TABLE I. Coulomb energy differences for  $A=209$  in keV.

Po-Bi	18.917 $\pm$ 33	Present
Bi-Pb	18.841 $\pm$ 10 <sup>a</sup>	b
	18.84 $\pm$ 20	c
	18.789 $\pm$ 7	d
	18.80 $\pm$ 20	e

<sup>a</sup>A previous result from Rutgers [D. J. Brendin, O. Hausen, G. Lenz, and G. M. Temmer, *Phys. Letters* **21**, 677 (1966)] gave a value of 18.98 MeV, but it is assumed that the more recent value is more accurate.

<sup>b</sup>G. H. Lenz and G. M. Temmer, *Nucl. Phys.* **A112**, 625 (1968).

<sup>c</sup>See Ref. 6.

<sup>d</sup>See Ref. 18.

<sup>e</sup>See Ref. 7.

tures between multiplets.<sup>2,4</sup> If such possible admixtures are neglected, the wave functions for the  $^{208}\text{Bi}$  states of interest here may be written as

$$\Psi_j^{j'j} = (\pi l'j', \nu l j^{-1})_j |c\rangle, \quad (3)$$

where  $l'j'$  refers to the  $h_{9/2}$  proton, and  $lj$  to the various neutron hole states, and  $|c\rangle$  refers to the  $^{208}\text{Pb}$  core. Similarly, if the ground state of  $^{209}\text{Bi}$  is taken as a  $h_{9/2}$  proton outside the  $^{208}\text{Pb}$  core, its analog in  $^{209}\text{Po}$  is

$$\Psi^{IAS} = \sum_{j \neq 9/2} \left( \frac{2j+1}{43} \right)^{1/2} (\pi l j, \nu l j^{-1})_0 \pi h_{9/2} |c\rangle + \delta_{j, 9/2} \left( \frac{9}{43} \right)^{1/2} (\pi l \frac{9}{2}, \nu l \frac{9}{2}^{-1})_0 \pi h_{9/2} |c\rangle. \quad (4)$$

According to a simple resonance theory of the nuclear reaction, the other nucleons are not affected by the emission of a proton from the analog resonance. The partial width for the decay of the analog resonance to a given excited state is expressed as a sum of terms, each being the product of a spectroscopic factor and a single-particle width for the emitted proton. The single-particle width is strongly dependent on the energy and angular momentum of the outgoing proton, because of the Coulomb and centrifugal barriers.

An analysis based on this theory has been used to obtain structure information in the lead region.<sup>18</sup> The single-particle widths were extracted from elastic and inelastic proton scattering from  $^{207}\text{Pb}$ .<sup>19,20</sup> If the  $^{208}\text{Pb}$  ground state is a doubly closed shell, and the low-lying states  $(l, j)$  in  $^{207}\text{Pb}$  are single-neutron holes in the  $(l, j)$  orbit, the observed partial widths are given by

$$\Gamma_{lj} = (2j+1/44) \Gamma_j^{sp}. \quad (5)$$

In the experiment reported here the simple shell-model estimates of the partial widths are

$$\Gamma_j^{j'j} = \frac{2j+1}{43(2j'+1)} \Gamma_j^{sp} \delta_{j'9/2}. \quad (6)$$

The  $\bar{p}$  cross section was then calculated using the expression

$$\frac{d\sigma}{d\Omega}(E\bar{p}) \propto \sum_i \frac{\Gamma_i}{(E-E_i)^2 + \frac{1}{4}\Gamma_i^2}, \quad (7)$$

where the sum extends over all states in the multiplets  $(\nu p_{1/2})^{-1}\pi h_{9/2}$ ,  $(\nu f_{5/2})^{-1}\pi h_{9/2}$ , and  $(\nu p_{1/2})^{-1}\pi h_{9/2}$ . The energies and spins of the states in  $^{208}\text{Bi}$  are taken from the  $^{209}\text{Bi}(d, t)$  experiment.<sup>2</sup>

In order to make the extracted single-particle

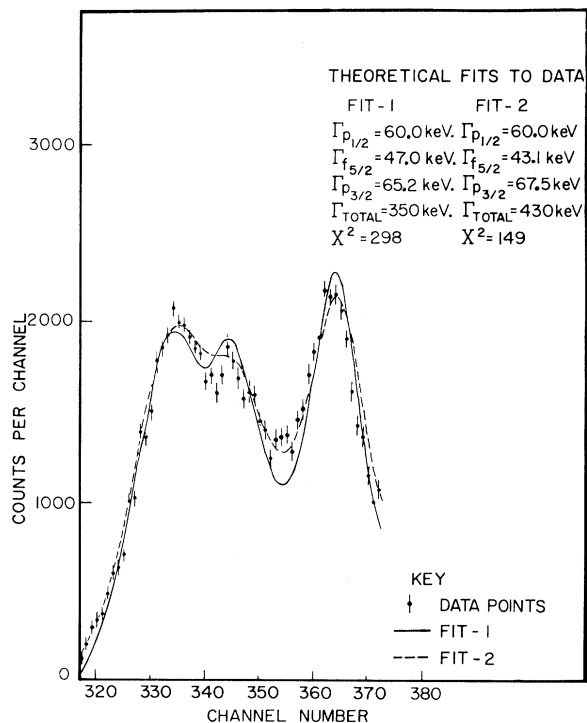


FIG. 4. A comparison of the theoretical fits to the data with background subtracted. Two curves calculated with different total widths are shown to illustrate the stability of the relative partial widths extracted.

widths directly comparable to the single-particle widths from the  $^{207}\text{Pb}$  proton scattering experiment, penetrability corrections have been made to the  $\Gamma_i$ 's appearing in Eq. (7). We replace  $\Gamma_i$  by  $\Gamma_i [P(E)/P(E_i)]$ , where  $E_i$  is the energy of the outgoing proton in the  $^{207}\text{Pb}$  (in) elastic scattering experiment at resonance, and  $P(E)$  is the penetrability calculated in the WKB approximation.

The procedure then was to subtract a smooth background from the experimental spectrum and do a least-squares fit to the remaining peaks,

TABLE II. Proton single-particle widths  $\Gamma_{ij}$  (keV).

	Present	$^{208}\text{Pb}(p, n\bar{p})^b$	$^{207}\text{Pb}(p, p)^c$	$^{207}\text{Pb}(p, p)^d$
$p_{1/2}$	60 <sup>a</sup>	60.5 ± 3.0	61 ± 15	66
$f_{5/2}$	43 ± 5	21 ± 2.4	17 ± 4	19
$p_{3/2}$	67 ± 5	69.2 ± 2.1	50 ± 11	44

<sup>a</sup>Normalized to 60 keV.

<sup>b</sup>See Ref. 9.

<sup>c</sup>G. M. Temmer, G. H. Lenz, and G. T. Garvey, in *Proceedings of International Conference on Nuclear Physics, Gatlingburg Tennessee, 12-17 September, 1966*, edited by R. L. Beeker and A. Zucker (Academic Press Inc., New York, 1967), p. 225.

<sup>d</sup>See Ref. 19.

varying the relative partial widths and gridding on the total width. The final widths were then obtained by normalizing  $\Gamma_{p_{1/2}}^{s,p}$  to 60 keV. Acceptable fits to the data for two different total widths are shown in Fig. 4. The relative partial widths are quite stable for different backgrounds and for a variation of the total width of up to 100 keV. However, for total widths smaller than 350 keV there is an excess of  $\bar{p}$  strength between the ground ( $h_{9/2}, p_{1/2}^{-1}$ ) and the ( $h_{9/2}, f_{5/2}^{-1}$ ) multiplet. The values for the proton widths extracted are shown in Table II. The errors quoted reflect the uncertainties associated with background subtraction and with the fitting procedure. The total width is not determined as accurately and, allowing for kinematic broadening, is given as  $380 \pm 80$  keV.

The relative widths extracted for the  $p_{1/2}$  and  $p_{3/2}$  channels agree reasonably well with the previous values obtained from other nuclei in this region, as shown in Table II. However the width for the  $f_{5/2}$  channel is considerably larger than previously observed.<sup>21</sup> Our results seem quite unambiguous, and in fact, a comparison with the  $\bar{p}$  spectrum from  $^{208}\text{Pb}(p, n\bar{p})$  shows that the  $f_{5/2}$  peak shown here is much stronger than the one extracted by Igo *et al.*<sup>9</sup> However, a recent preliminary result<sup>22</sup> on  $^{208}\text{Pb}(p, n\bar{p})$  confirms the larger  $f_{5/2}$  width. The value of the total width of the analog state is also larger for  $^{209}\text{Bi}$  than for  $^{208}\text{Pb}$ , but this may only reflect a difference in the mixing with the background levels.

A calculation is currently in progress taking into account the effect of the residual interaction on the partial widths.<sup>23</sup>

#### 5. $^{209}\text{Bi}(p, d)^{208}\text{Bi}$

The  $^{209}\text{Bi}(p, d)^{208}\text{Bi}$  reaction was measured simultaneously with the ( $p, n\bar{p}$ ) experiment, and it also reaches the same final states in  $^{208}\text{Bi}$ . The thick-target spectrum shown in Fig. 5 shows the multiplet structure extending up to the ( $h_{9/2}, h_{9/2}^{-1}$ ) multiplet. A thin-target spectrum with good resolution is also shown in Fig. 5. The angular distributions are in good agreement with the  $l$  assignments from the ( $d, t$ ) reaction.<sup>2</sup>

#### 6. CONCLUSIONS

The proton reduced widths extracted from the  $^{209}\text{Bi}(p, n\bar{p})$  experiment agree with the values extracted both from resonance experiments and the  $^{208}\text{Pb}(p, n\bar{p})$  experiment for the  $p_{1/2}$  and  $p_{3/2}$  shells. However, there is a marked disagreement for the  $f_{5/2}$  shell. A total width of 380 keV was also obtained for the analog state, and the  $^{209}\text{Pb}$ - $^{209}\text{Bi}$  Coulomb energy difference was  $18.92 \pm 0.03$  MeV.

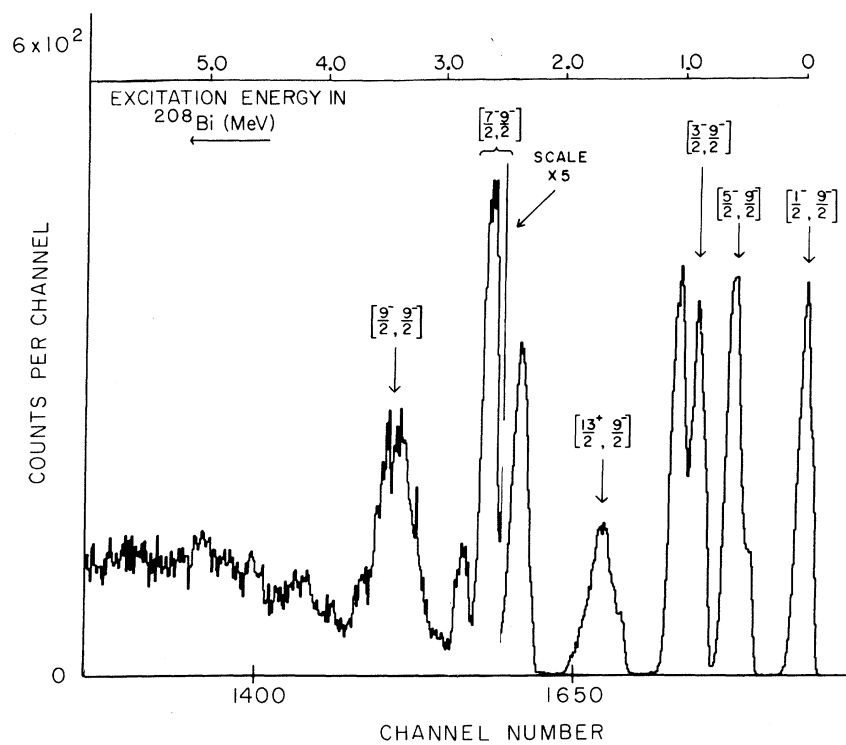
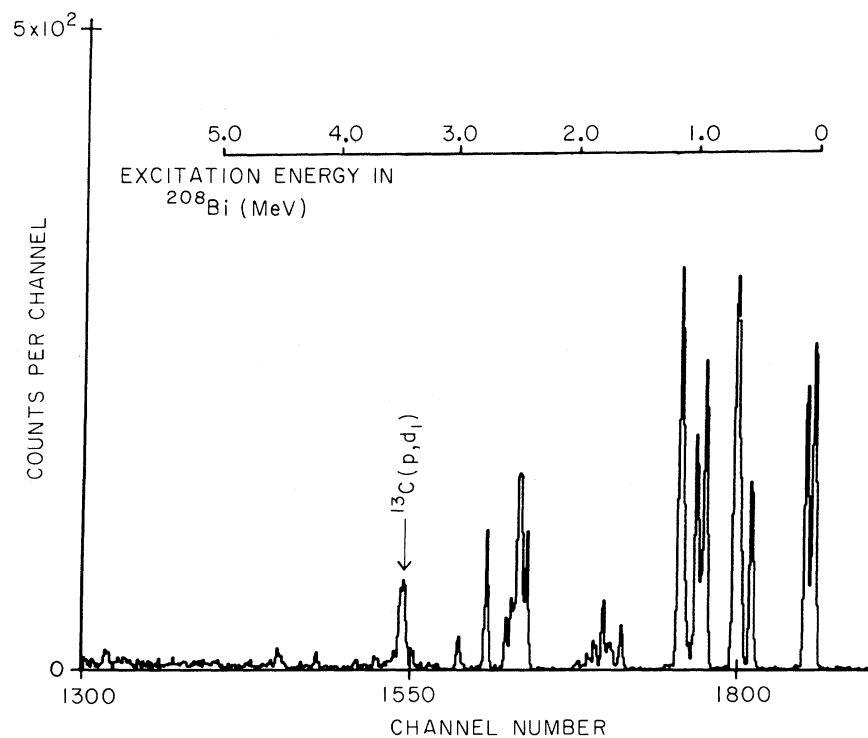


FIG. 5. (a)  $^{209}\text{Bi}(p, d)^{208}\text{Bi}$  spectrum with a thin target and (b)  $^{209}\text{Bi}(p, d)^{208}\text{Bi}$  with a thick target. The close multiplet structure of  $^{208}\text{Bi}$  up to  $(h_{9/2}h_{9/2}^{-1})$  is clearly seen in the thick-target spectrum.

†Research supported in part by the National Science Foundation.

<sup>4</sup>G. Muehlelehner, A. S. Poltorak, W. C. Parkinson, and R. H. Bassel, *Phys. Rev.* **159**, 1039 (1967); W. P. Alford and D. G. Burke, *Phys. Rev.* **185**, 1560 (1969); G. R. Satchler, W. C. Parkinson, and D. L. Hendrie, *Phys. Rev.* **187**, 1491 (1969).

<sup>2</sup>Y. E. Kim and J. O. Rasmussen, *Phys. Rev.* **135**, B44 (1964).

<sup>3</sup>J. R. Erskine, *Phys. Rev.* **135**, B110 (1964).

<sup>4</sup>W. P. Alford, J. P. Schiffer, and J. J. Schwartz, *Phys. Rev. Letters* **21**, 156 (1968); W. P. Alford, private communication.

<sup>5</sup>P. Richard, W. G. Weitkamp, W. Wharton, H. Wieman, and P. von Brentano, *Phys. Letters* **26B**, 8 (1967).

<sup>6</sup>C. D. Kavaloski, J. S. Lilley, P. Richard, and N. Stein, *Phys. Rev. Letters* **16**, 807 (1966).

<sup>7</sup>C. F. Moore, L. J. Parish, P. von Brentano, and S. A. A. Zaidi, *Phys. Letters* **22**, 616 (1966).

<sup>8</sup>G. Ballois, J. Saudinos, O. Beer, M. Gendrot, and P. Lopato, *Phys. Letters* **22**, 659 (1966).

<sup>9</sup>G. J. Igo, C. A. Whitten, Jr., Lean-Luc Perreouud, J. W. Verba, T. J. Woods, J. C. Young, and L. Welch, *Phys. Rev. Letters* **22**, 724 (1969).

<sup>10</sup>A. I. Yavin, R. A. Hoffswell, L. H. Jones, and T. M. Noweir, *Phys. Rev. Letters* **16**, 1049 (1966).

<sup>11</sup>P. S. Miller, Princeton University Technical Report

No. PUC-937-339, 1968 (unpublished).

<sup>12</sup>P. S. Miller and G. T. Garvey, to be published.

<sup>13</sup>D. L. Bayer and W. Benenson, *Bull. Am. Phys. Soc.* **14**, 1243 (1969).

<sup>14</sup>E. Kashy, MSUCL Internal Report, 1969 (unpublished).

<sup>15</sup>C. Maples, G. W. Goth, and J. Cerny, University of California Lawrence Radiation Laboratory Report No. UCRL-16964 (unpublished).

<sup>16</sup>J. D. Anderson, C. Wong, and J. W. McClure, *Phys. Rev.* **138**, B165 (1965).

<sup>17</sup>N. Auerbach, J. Hufner, A. K. Kerman, and C. M. Shakin, *Phys. Rev. Letters* **23**, 484 (1969).

<sup>18</sup>W. R. Wharton, P. von Brentano, W. K. Dawson, and P. Richard, *Phys. Rev.* **176**, 1424 (1968).

<sup>19</sup>B. L. Anderson, J. P. Bondorf, and B. S. Madsen, *Phys. Letters* **22**, 651 (1966).

<sup>20</sup>C. J. Batty, B. Bommer, E. Freidman, C. T. Schaler, A. S. Cloagh, J. B. Hunt, and L. E. Williams, *Nucl. Phys.* **A116**, 643 (1968).

<sup>21</sup>P. Richard, in *Nuclear Isospin*, edited by J. D. Anderson, S. D. Bloom, J. Cerny, and W. W. True (Academic Press Inc., New York, 1969), p. 547 and Refs. therein.

<sup>22</sup>G. M. Crawley, P. S. Miller, and D. L. Bayer, *Bull. Am. Phys. Soc.* **15**, 626 (1970).

<sup>23</sup>S. A. A. Zaidi and P. Dyer, *Phys. Rev.* **185**, 1332 (1969).

## Experimental Studies of Neutron-Deficient Gadolinium Isotopes.

### I. The Electron-Capture Decay of $\text{Gd}^{149}$

R. E. Eppley and Wm. C. McHarris

*Department of Chemistry\* and Cyclotron Laboratory, † Department of Physics, Michigan State University, East Lansing, Michigan 48823 and*

W. H. Kelly

*Cyclotron Laboratory, † Department of Physics, Michigan State University, East Lansing, Michigan 48823*

(Received 16 March 1970)

$\gamma$  rays emitted in 9.4-day  $\text{Gd}^{149}$  have been studied with  $\text{Ge}(\text{Li})$  and  $\text{NaI}(\text{Tl})$  detectors. 25  $\gamma$  rays have been attributed to the decay of  $\text{Gd}^{149}$  with energies and relative intensities of 149.6 (233), 214.5 (0.81), 252.3 (1.1), 260.5 (5.8), 272.0 (15), 298.5 (127), 346.5 ( $\approx 100$ ), 405.5 (3.7), 430 (0.33), 459.9 (2.4), 478.7 (0.95), 496.4 (7.2), 516.4 (11), 534.2 (13), 645.2 (5.9), 663.3 (1.1), 666.2 (3.9), 748.2 (35), 788.6 (30), 812.4 (0.55), 863 (0.32), 875.8 (0.90), 933.3 (2.2), 939.1 (9.0), and 947.7 keV (3.7). On the basis of coincidence and anticoincidence experiments, relative intensities, and energy sums, states in  $\text{Eu}^{149}$  have been placed at 0, 149.6, 459.9, 496.2, 534.2, 666.0, 748.2, 794.8, 812.4, 875.8, 933.3, 939.1, and 1097.3 keV. The  $\text{Eu}^{149}$  x-ray intensity has also been measured. From our  $\gamma$ -transition intensities and published conversion-electron intensities, conversion coefficients were obtained for most of the electro-magnetic transitions, thus allowing multipolarity assignments to be made for these transitions. These assignments, together with the  $\log ft$  values, were then used for the placement of limits on the spins of the deduced levels. Our proposed decay scheme is compared with previously published decay schemes and is discussed in terms of current models.

#### I. INTRODUCTION

Neutron-deficient Gd isotopes lie in a region of special interest for the testing of nuclear models.

They and their Eu daughters range from nuclei that have large quadrupole moments, suggesting permanently deformed nuclei, through closed-shell nuclei that can be described by an extreme single-